Thermodynamic observation of first-order vortex-lattice melting transition in $Bi_2Sr_2CaCu_2O_8$

E. Zeldov*, D. Majer*, M. Konczykowski†, V. B. Geshkenbein‡§, V. M. Vinokur¶ & H. Shtrikman*

* Department of Condensed Matter Physics, The Weizmann Institute of Science, 76100 Rehovot, Israel
† Centre d'Études et de Recherches sur les Matérieux, Laboratoire des Solides Irradiés, École Polytéchnique, 91128 Palaiseau, France
‡ Theoretische Physik, ETH-Hönggerberg, CH-8093 Zürich, Switzerland
§ L. D. Landau Institute for Theoretical Physics, 117940 Moscow, Russia
¶ Argonne National Laboratory, Argonne, Illinois 60439, USA

The lattice of magnetic flux lines that can permeate a type II superconductor, such as the high-transition-temperature copper oxide materials, melts from a solid-like state to a liquid-like state at a temperature below the superconducting transition temperature. Contrary to the predictions of mean-field theory, this phase transition in $Bi_2Sr_2CaCu_2O_8$ is found to be first-order. The vortex liquid discontinuously expands on freezing.

THE discovery of high-transition-temperature (high-T_c) superconductors has revived the interest in study of the nature of the mixed state, where superconductivity coexists with the inhomogeneous magnetic field inside the material. Magnetic fields penetrate conventional type II superconductors in the form of a periodic array of vortices or flux lines known as the Abrikosov lattice[1]. The temperature-dependent critical fields $H_{c1}(T)$ and $H_{c2}(T)$ confine the domain of the mixed state on the H–T phase diagram. Fields above H_{c2} destroy superconductivity, whereas fields below H_{c1} at the surface of a sample do not penetrate into the bulk of the material.

In high-T_c superconductors the combination of high operating temperature, short superconducting coherence length and high anisotropy enormously enhances the role of thermal fluctuations of the flux lines, resulting in a noticeable change in the nature of the mixed state. The most important effect of thermal fluctuations is the possibility of melting of the vortex lattice at temperatures well below the superconducting transition temperature[2,3]. The resulting vortex-liquid phase may occupy a significant part of the H–T phase diagram[4]. In addition, the inevitable presence of defects and disorder in the material gives rise to pinning of the flux lines, which enriches the variety of different possible vortex states. In particular, it has been demonstrated that quenched disorder drives the vortex lattice into a vortex-glass state[5–8]. It is now believed that the freezing of the vortex liquid into a disordered vortex solid in sufficiently impure high-T_c superconductors crystals occurs via a continuous second-order phase transition[4–6].

On the other hand, it was suggested[9] that the mean-field formation of the vortex lattice at H_{c2}, which occurs via a thermodynamic second-order transition, can be driven first-order by the superconducting fluctuations. One may therefore expect that in sufficiently clean crystals the vortex liquid freezes into a solid through a thermodynamic first-order phase-transition.

Additional effects may arise from the layered structure of high-T_c superconductors. In layered materials, vortex-lattice melting may occur in two separate stages: the melting of the vortex lattice into a liquid of vortex lines, and the subsequent loss of coherence between the layers—the decoupling transition[10–12]. At moderate anisotropy the decoupling of a vortex-line liquid into a liquid of two-dimensional pancake vortices can be a first-order phase transition as well[12].

The structure of the different possible vortex states and the nature of the thermodynamic transitions between the phases has become one of the central questions of the physics of the mixed state and has attracted much recent attention[13–15]. In view of the traditional mean-field prediction of a second-order phase transition[1], the possibility of a thermodynamic first-order transition of the vortex-lattice is of fundamental interest[4]. Experimentally, the main evidence for the existence of first-order melting has been drawn from the observation of sharp kinks in the resistive transition of clean $YBa_2Cu_3O_7$ (YBCO) crystals[16–21]. However, resistivity is not a thermodynamic property, and this kink reflects a change in vortex dynamics that does not necessarily mark a transition between distinct thermodynamic phases. At the same time, a true first-order phase transition should have clear thermodynamic features: latent heat and a discontinuous step in specific volume or density. In addition, one would expect a similar behaviour in all high-T_c superconductor materials, not only in YBCO. Recently, vortex-lattice melting in $Bi_2Sr_2CaCu_2O_8$ (BSCCO) was inferred from disappearance of the neutron diffraction pattern at elevated temperatures[15]. This result implies that a vortex-liquid phase occupies a significant part of the H–T phase diagram of BSCCO; however, the order of the phase transition between the solid and the liquid phases cannot be determined. A thermodynamic indication of a possible first-order transition was recently obtained by magnetic measurements on BSCCO crystal[22]. Owing to limited resolution, however, the observed change in magnetization was relatively broad and not well quantified.

Here we present a very clear and direct thermodynamic observation of a first-order phase transition of the vortex lattice by use of local vortex-dynamics measurements. The local field, B, shows a discontinuous step at the transition, analogous to the discontinuous change in the specific volume on melting of a regular solid. The sensitivity of our measurement allows an accurate mapping of the melting line and the associated entropy change.

Experimental details

It was shown previously[23,24] that the magnetic field B inside a platelet crystal is not uniform even at equilibrium magnetization. This situation is comparable to a regular solid under non-uniform pressure across the sample. As a result, the vortex-lattice melting transition occurs at a slightly different temperature or applied field at various positions inside the superconductor sample. Therefore the signal integrated over the entire sample in a standard global magnetization measurement will display a

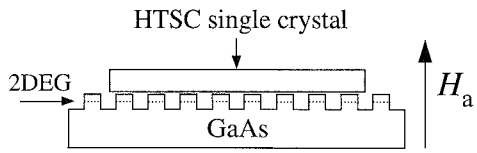

FIG. 1 Schematic diagram of the experimental setup (not to scale). An array of ten sensors with an active area of $3\times3\ \mu m^2$ each, is etched in a GaAs/AlGaAs heterostructure. A superconductor crystal is put directly on the surface of the probes. The two-dimensional electron-gas (2DEG) active layer resides only ~1,000 Å below the surface. As a result a very accurate measurement of the local magnetic field is obtained at each of the sensor locations across the crystal.

significantly broader and smoother transition compared with the underlying physical mechanism. To probe the true width of the phase transition, local measurements with high spatial resolution are therefore required. For this purpose we have used an array of microscopic Hall sensors realized in a two-dimensional electron gas formed at a GaAs/AlGaAs interface as shown schematically in Fig. 1. A high-quality BSCCO crystal of $\sim0.7\times0.3\times0.1\ mm^3$ ($T_c=90$ K) was put directly onto the surface of the sensors, and a perpendicular external magnetic field, $H_a\|z\|c$-axis was applied. The Hall-sensor array allows the study of local vortex behaviour with high field sensitivity and high spatial resolution as demonstrated below. An additional advantage of this technique is that the actual value of the local B_z is obtained. In global magnetization measurements only the value of the applied field H_a is known, and an accurate evaluation of B is difficult owing to complicated demagnetization effects and not well known critical field values.

The phase transition

A first-order phase transition is associated with a discontinuous step in density. Because each vortex carries a magnetic flux, a step in vortex density is identical to a step in the local macroscopic magnetic field. Hence, by a careful measurement of the local B_z at the surface of the sample, we can directly observe the thermodynamic discontinuous change in the vortex density at the phase transition. This discontinuity should occur as the transition line is crossed either by sweeping the applied field or by sweeping the temperature. We have carried out measurements in both regimes. Figure 2 shows the discontinuous step in B_z as the applied field is increased at a constant temperature of 80 K. The width of the transition is less than 0.4 Oe. This step occurs at the same thermodynamic value of the local B_z at various locations across the sample, but at different values of H_a owing to the non-uniform B_z profile[23,24].

Figure 3 shows two examples of temperature sweeps at constant fields of $H_a=53$ and 240 Oe. The observed transition is extremely sharp. In most of our measurements the entire transition occurs between two adjacent measurements. The width of the transition is therefore less than our temperature resolution of about 1 mK. Such a discontinuous step in vortex density is a clear thermodynamic demonstration of a first-order phase transition. It is important to note that B_z in the liquid phase above the transition is higher than in the solid phase, which means that the vortex liquid is denser than the vortex solid, in contrast to the common behaviour of solids. Thus the vortex-liquid is similar to water, which expands on freezing into ice. Such behaviour is in fact consistent with equation (1) below. On increasing the temperature a small hysteresis is observed with a slightly rounded transition that looks very similar to the reported resistive hysteresis in untwinned YBCO crystals[18,20]. The controversial origin of the hysteresis[20] requires further investigation of this effect. As an example of the sensitivity of our measurement, at 240 Oe there are about 100 vortices in the area of each Hall sensor, and the measured step in B_z corresponds approximately to an addition of only 0.1 vortex to the area.

The resulting vortex-lattice melting line, $B_m(T)$, is shown in Fig. 4. The squares are points obtained by temperature sweeps, and the circles are the field sweep results. The existing theoretical derivations of the vortex-lattice melting line based on the Lindemann criterion[25–28] predict a power-law behaviour that can be approximated by $B_m(T)=B_0(1-T/T_c)^\alpha$, where $\alpha\leqslant2$. The solid curve in Fig. 4 is a best fit to the data, which results in $\alpha=1.55$, $B_0=990$ G, and $T_c=94.2$ K. The power law fit describes well the behaviour in the central region; however, there are significant deviations at both high and low temperatures. On the other hand, the vortex-line liquid to vortex-pancake liquid decoupling line is expected to follow[11,12] $B_D(T)\approx B_0(T_c-T)/T$, with $B_0\approx\alpha_D\varepsilon^2\phi_0^3/(4\pi\lambda(0))^2T_cd$. Here $\alpha_D\approx0.1$ is a universal constant, $d=15$ Å is the interlayer spacing, $\lambda(0)\approx2{,}000$ Å is the penetration length, and ε is the anisotropy ratio. A fit to the experimental data (dashed curve in Fig. 4) results in a better agreement at high temperatures, with a more realistic $T_c=90.9$ K and $B_0=400$ G. Using the above parameters we obtain $\varepsilon^{-1}\approx140$, which is consistent with existing estimates[29].

At lower temperatures, the melting line shows a rather sudden flattening, in contrast with the theoretically predicted behaviour[11,12,25–28]. However, the most striking feature of $B_m(T)$ is the existence of a well-defined critical point at a characteristic temperature of 37.8 K and field of 380 G, beyond which no discontinuous transition is observed. Figure 5 shows the measured height of the discontinuous step at the transition, ΔB, along the melting line. We have carefully measured ΔB in the vicinity of the critical point by temperature sweeps at constant H_a, and have changed H_a by small increments. ΔB is very well resolved at fields below the critical point. However, when H_α is increased only by 1 Oe above the critical point, ΔB disappears completely. The step height ΔB increases monotonically with T_m and reaches a maximum value of about 0.4 G at $T_m\approx83$ K. At higher temperatures ΔB drops rapidly as T_m approaches T_c. The reason for this general form of $\Delta B(T_m)$ is not obvious.

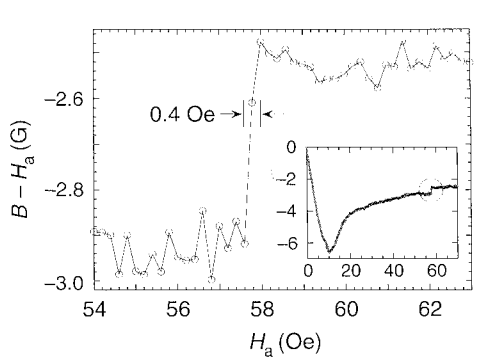

FIG. 2 Step in the local field, B, as the melting line is crossed by increasing the applied field at 80 K. Solid line is guide for the eye. The inset shows the entire local magnetization curve, $B-H_a$, as a function of increasing applied field H_a. The melting transition region is encircled.

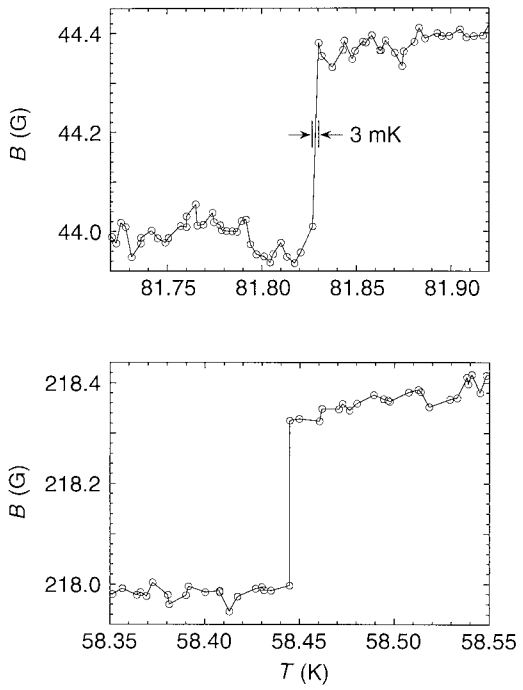

FIG. 3 Two examples of the step in local B on crossing the melting line by decreasing the temperature at constant applied fields of 53 Oe (top panel) and 240 Oe (bottom panel). Solid lines are guides for the eye. The sample was cooled very slowly, at a typical rate of 5 to 15 mK min^{-1}, while B_z and T were measured at constant time intervals.

Using the Clausius–Clapeyron relations we can calculate the entropy change at the transition and the latent heat per unit volume

$$\Delta S = -\frac{\Delta B}{4\pi}\frac{dH_m}{dT} \qquad L = T_m \Delta S \tag{1}$$

The entropy change per vortex per CuO layer is therefore given by

$$\Delta s = -\frac{d\phi_0}{4\pi}\frac{\Delta B}{B_m}\frac{dH_m}{dT} \tag{2}$$

In platelet geometry the field, H, is generally not known; it is position dependent and differs from H_a. Because in our case $B_m(T) \gtrsim H_{c1}(T)$, we can approximate dH_m/dT in equations (1) and (2) by dB_m/dT, which is measured directly with high precision. The resulting Δs is shown in Fig. 6. Close to T_c the entropy change per vortex increases rapidly with temperature, which could be related to critical fluctuations. Note that ΔS per unit volume approaches zero at T_c; however, at high temperatures B_m decreases faster than ΔB, which results in Δs increasing with temperature as determined by equation (2). Close to T_c the error bar in Δs is large and it is plausible that Δs does eventually vanish at T_c.

At lower temperatures, $T_m < 75$ K, the entropy change, Δs, decreases linearly with decreasing temperature and vanishes at the critical point as it should. But one would expect a continuous vanishing of ΔB as well. In contrast, ΔB seems to remain finite at temperatures above the critical point, as shown in Fig. 5, and we could not detect any gradual disappearance of the field step. The continuous vanishing of ΔS, however, is determined by the vanishing of dB_m/dT due to the flattening of $B_m(T)$ close to the critical point (see Fig. 4), and not by the vanishing of ΔB as expected. The existence of the critical point is possibly disorder-related, in which case at lower temperatures a second-order melting line should continue from this tricritical point. This feature was observed previously[21] in YBCO crystals by using resistive measurements. The position of the critical point was reported to shift to lower fields with increasing disorder (D. J. Bishop, personal communication).

Discussion

The latent heat and ΔB can be estimated as follows. At the melting temperature the free energies F of the solid and the liquid phases are equal and hence $\Delta F = \Delta U - T_m \Delta S = 0$. The energy required to transform a unit volume of a vortex solid into a liquid is estimated as $\Delta U \approx c_L^2 c_{66}$. Here $c_{66} \approx \phi_0 B_m/(8\pi\lambda)^2$ is the shear modulus of the vortex solid that vanishes in the liquid phase, and $c_L \approx 0.2$ is the Lindemann number. As a result, $\Delta S \simeq c_L^2 c_{66}/T_m$. Making use of the estimate of the melting temperature[4] $T_m \approx 10.8 c_L^2 c_{66} \varepsilon a_0^3$, where $a_0 = (\phi_0/B_m)^{1/2}$ is the intervortex spacing, one can evaluate[30] the entropy change per vortex per layer as $\Delta s \approx (0.1 d/\varepsilon)(B_m/\phi_0)^{1/2}$. Accordingly, $\Delta B \approx -(0.4\pi/\varepsilon)(B_m/\phi_0)^{3/2}/(dB_m/dT)$. Using the theoretical T_m and taking $\lambda(0) = 2{,}000$ Å, we find $\Delta B \approx 0.2$ G at low temperatures, which compares favourably with the experimental results.

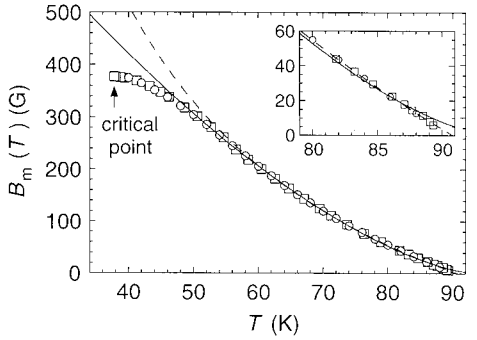

FIG. 4 First-order phase-transition line in BSCCO as measured by field scans (○) and temperature scans (□). The solid line is a fit to $(1 - T/T_c)^{\alpha}$ vortex-lattice melting transition behaviour; the dashed line is a fit to the $(T_c - T)/T$ decoupling transition. Inset: phase-transition line $B_m(T)$ in the vicinity of T_c.

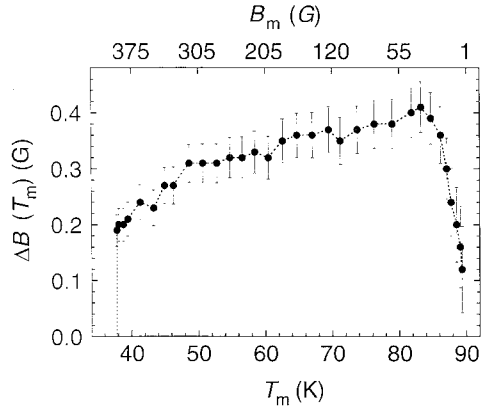

FIG. 5 The height of the field step at the melting transition as a function of the melting temperature, T_m, as derived from the temperature scans as in Fig. 3. Field scans yield very similar results. The dashed line is a guide for the eye. The field step disappears below the critical point. The corresponding approximate B_m values are shown along the top.

Note, however, that the above analysis results in $\Delta s(T) \propto (1 - T/T_c)$ close to T_c and apparently does not describe the observed increase in Δs with temperature. The resulting temperature behaviour of $\Delta B \propto (1 - T/T_c)^2$ seems to overestimate the observed rate of decrease in ΔB with temperature close to T_c.

As mentioned above, another possible origin of the observed effects is the decoupling transition. Although giving somewhat better consistency with the experimental observations, this model cannot explain the overall temperature dependence of ΔB and Δs as well. In this case the energy necessary to decouple a unit volume of the vortex-line liquid is $\Delta U \approx E_J/2d$, where $E_J \approx a_D \varepsilon^2 \phi_0^2/(4\pi\lambda)^2 d$ is the Josephson coupling energy between layers per unit area, and the decoupling temperature is $T_D \approx E_J a_0^2$ (refs 4, 11). Proceeding as above we obtain straightforwardly $\Delta S \approx 1/2a_0^2 d$, and a temperature-independent $\Delta s \approx 0.5 k_B$ (ref. 12). Near T_c we find $\Delta B \approx 2\pi(T_c - T)/\phi_0 d$, yielding $\Delta B \approx 0.3$ G at 80 K, and $\Delta B \approx 2\pi T_D/\phi_0 d$ at low temperatures. However, the neutron diffraction data[15] seem to favour the melting interpretation. The data indicate the presence of an ordered state at lower temperatures and the disappearance of long-range order at the transition. It is quite plausible, however, that the melting and decoupling transitions occur simultaneously or quite close to each other at low fields in BSCCO[31].

In Monte-Carlo simulations of vortex-lattice melting[32] $\Delta s \approx 0.3 k_B$ was obtained, which is within the bulk of our data. These calculations were carried out in the high-field regime of $a_0 \ll \lambda$ and cannot be directly applied to our low-field case. The previously evaluated $\Delta s \approx 0.06 k_B$ in BSCCO at 220 Oe (ref. 22) is significantly lower than our result of $0.28 \pm 0.03 k_B$ reported here at the same field. Another point of reference is the melting of usual solids. In metals a typical value of the latent heat is $1\ k_B T_m$ per atom. In BSCCO at $T_m = 83$ K, for example, $1\ k_B T_m$ of energy per vortex per layer is similarly required to melt the vortex lattice (although for vortex lines the characteristic vortex length is εa_0 and not d as in the decoupling case). However, in regular solids the density of the solid cannot be changed substantially by changing the pressure. The density of the vortex lattice, in contrast, changes by orders of magnitude along the melting line of Fig. 4. The associated latent heat per vortex is also changing by orders of magnitude from zero at high vortex densities to substantial values at low vortex densities close to T_c.

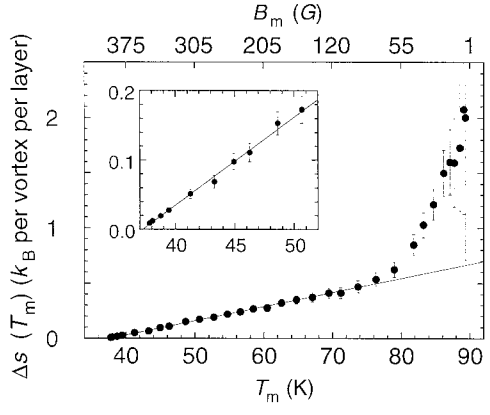

FIG. 6 Entropy change per vortex per layer at the melting transition as a function of T_m. Inset: expanded view near the critical point. Solid lines show linear fit to the data.

We note that in YBCO the vortex solid is pinned and finite critical currents exist below $B_m(T)$, which cause the observed step in resistivity at the melting transition[16-21]. In BSCCO, in contrast, the vortices are unpinned below the transition at elevated temperatures[24], and such a resistive step should therefore not be observable, consistent with the experimental results[33]. On the other hand, in YBCO it would be very difficult to observe the field step owing to the small $\Delta B/B_m$ ratio and because of vortex pinning below the transition.

Another interesting point is that the observed phase transition in BSCCO occurs at fields that are three orders of magnitude below the mean-field transition at H_{c2}, demonstrating the enhanced role of thermal fluctuations. The theoretical estimates on the basis of the vortex-lattice melting and decoupling transition models give $\Delta B \approx 0.5$ G, in reasonable agreement with the data, but neither of the existing theories can fully describe the temperature dependencies of $B_m(T)$ and $\Delta B(T)$. □

Received 9 February; accepted 27 April 1995.

1. Abrikosov, A. A. *Zh. eksp. teor. Fiz.* **32,** 1442–1452 (1957) [*Soviet Phys. JETP* **5,** 1174–1182 (1957)].
2. Bishop, D. J., Gammel, P. L., Schneemeyer, L. F. & Waszczak, J. V. *Bull. Am. phys. Soc.* **33,** 606 (1988).
3. Nelson, D. R. *Phys. Rev. Lett.* **60,** 1973–1976 (1988).
4. Blatter, G., Feigel'man, M. V., Geshkenbein, V. B., Larkin, A. I. & Vinokur, V. M. *Rev. mod. Phys.* **66,** 1125–1388 (1994).
5. Fisher, M. P. A. *Phys. Rev. Lett.* **62,** 1415–1418 (1989).
6. Fisher, D. S., Fisher, M. P. A. & Huse, D. A. *Phys. Rev.* B**43,** 130–159 (1991).
7. Larkin, A. I. *Zh. eksp. teor. Fiz.* **58,** 1466–1470 (1970) [*Soviet Phys. JETP* **31,** 784–786 (1970)].
8. Vinokur, V. M., Feigel'man, M. V., Geshkenbein, V. B. & Larkin, A. I. *Phys. Rev. Lett.* **65,** 259–262 (1990).
9. Brezin, E., Nelson, D. R. & Thiaville, A. *Phys. Rev.* B**31,** 7124–7131 (1985).
10. Feigel'man, M. V., Geshkenbein, V. B. & Larkin, A. I. *Physica* C**167,** 177–187 (1990).
11. Glazman, L. I. & Koshelev, A. E. *Phys. Rev.* B**43,** 2835–2843 (1991).
12. Daemen, L. L., Bulaevskii, L. N., Maley, M. P. & Coulter, J. Y. *Phys. Rev. Lett.* **70,** 1167–1170 (1993); *Phys. Rev.* B**47,** 11291–11301 (1993).
13. Huse, D. A., Fisher, M. P. A. & Fisher, D. S. *Nature* **358,** 553–559 (1992).
14. Bishop, D. J., Gammel, P. L., Huse, D. A. & Murray, C. A. *Science* **255,** 165–172 (1992).
15. Cubitt, R. *et al. Nature* **365,** 407–411 (1993).
16. Safar, H. *et al. Phys. Rev. Lett.* **69,** 824–827 (1992).
17. Kwok, W. K. *et al. Phys. Rev. Lett.* **69,** 3370–3373 (1992).
18. Kwok, W. K. *et al. Phys. Rev. Lett.* **72,** 1092–1095 (1994).
19. Charalambous, M., Chaussy, J., Lejay, P. & Vinokur, V. *Phys. Rev. Lett.* **71,** 436–439 (1993).
20. Jiang, W., Yeh, N.-C., Reed, D. S., Kriplani, U. & Holtzberg, F. *Phys. Rev. Lett.* **74,** 1438–1441 (1994).
21. Safar, H. *et al. Phys. Rev. Lett.* **70,** 3800–3803 (1993).
22. Pastoriza, H., Goffman, M. F., Arribere, A. & de la Cruz, F. *Phys. Rev. Lett.* **72,** 2951–2954 (1994).
23. Zeldov, E. *et al. Phys. Rev. Lett.* **73,** 1428–1431 (1994).
24. Zeldov, E. *et al. Europhys. Lett.* **30,** 367–372 (1995).
25. Houghton, A., Pelcovits, R. A. & Sudbo, A. *Phys. Rev.* B**40,** 6763–6770 (1989).
26. Brandt, E. H. *Phys. Rev. Lett.* **63,** 1106–1109 (1989).
27. Hikami, S., Fujita, A. & Larkin, A. I. *Phys. Rev.* B**44,** 10400–10403 (1991).
28. Blatter, G. & Ivlev, B. I. *Phys. Rev.* B**50,** 10272–10286 (1994).
29. Martinez, J. C. *et al. Phys. Rev. Lett.* **69,** 2276–2279 (1992).
30. Geshkenbein, V. B., Ioffe, L. B. & Larkin, A. I. *Phys. Rev.* B**48,** 9917–9920 (1993); *Physica* A**200,** 278–286 (1993).
31. Sasik, R. & Stroud, D. *Phys. Rev.* B (in the press).
32. Hetzel, R. E., Sudbo, A. & Huse, D. A. *Phys. Rev. Lett.* **69,** 518–521 (1992).
33. Safar, H., Gammel, P. L., Bishop, D. J., Mitzi, D. B. & Kapitulnik, A. *Phys. Rev. Lett.* **68,** 2672–2675 (1992).

ACKNOWLEDGEMENTS. We thank H. Motohira for providing the BSCCO crystal. We also thank A. I. Larkin, A. E. Koshelev, V. G. Kogan, G. Blatter and V. Steinberg for their comments. This work was supported by the Israeli Ministry of Science and the Arts, by the Glikson Foundation, by the Minerva Foundation, and by France–Israel cooperation programme PICS 112. V.M.V. received support from the US DoE, BES-Materials Sciences, and the Albert Einstein Minerva Centre for Theoretical Physics at the Weizmann Institute of Science. V.B.G. received support from ISF and from the Einstein Minerva Centre.